RJC

RASĀYAN *J. Chem.*
Vol. 8 | No.4 |490 - 508 | October - December | 2015
ISSN: 0974-1496 | e-ISSN: 0976-0083 | CODEN: RJCABP
http://www.rasayanjournal.com
http://www.rasayanjournal.co.in

MOLECULAR STRUCTURE, SPECTROSCOPIC STUDIES, HOMO-LUMO PROFILE AND NBO ANALYSIS OF 3-ETHOXY-4-HYDROXY BENZALDEHYDE

T.Chithambarathanu[1,*], K.Vanaja[2] and J. Daisy Magdaline[2]
[1,*]Department of Physics, S.T.Hindu College, Nagercoil (T.N) India
[2]Department of Physics, Rani Anna Government Arts College for women, Tirunelveli (T.N) India
[*]E-mail: tchithambarathanu@gmail.com

ABSTRACT

The geometric parameters and theoretical vibrational frequencies of 3-Ethoxy-4-hydroxybenzaldehydeare calculated using HartreeFock (HF)method with 6-31G(d,p) basis set and Density functional theory (B3LYP) methods with 6-31++G(d,p) and6-311++G(d,p) basis sets. The detailed interpretation of the vibrational spectra has been carried out with the aid of normal coordinate analysis following the scaled quantum mechanical force field methodology (SQM). The UV absorption spectra of the title compound in the solvents, water and ethanol, are recorded in the range of 200-400 nm. NBO analysis is also carried out to find out the intra-molecular electronic interactions and their stabilization energy. The highest occupied molecular orbital (HOMO) and lowest unoccupied molecular orbital (LUMO) energies are also found. Thermodynamic properties like entropy, heat capacity and zero point energy have been calculated for the title molecule. The Molecular Electrostatic Potential (MESP) analysis reveals the sites for electrophilic attack and nucleophilic reactions in the molecule.

Keywords: 3-Ethoxy-4-hydroxy benzaldehyde, Density functional theory, HOMO, LUMO, FT-IR, FT-Raman

INTRODUCTION

3-Ethoxy-4-hydroxy benzaldehyde (EHB) is commonly known as ethyl vanillin, which is atrisubstituted benzene with -CHO, $-OCH_2CH_3$ and -OH groups substituted at 1, 3, 4 positions of the ring. Ethyl vanillin is a chemically synthesized flavouring agent related to vanillin or artificial vanilla. Ethyl vanillin is widely used as a fragrance in cosmetics and as a flavour enhancer in food production (chocolate, candies, biscuits, instant noodles and bread), beverage and animal feed. It is also used in the electroplating industry, and as a brightener to whiten paper and fabric. Ethyl vanillin is used as an intermediate reagent in the synthesis of many drugs.

The vibrational spectra of the 3-methoxy-4-hydroxybenzaldehyde (vanillin) had already been interpreted by Gunasekaran and Ponnusamy[1] on the basis of normal coordinate analysis. Several vibrational spectroscopic studies on mono-, di-, tri- substituted benzaldehydes have been reported[2-7].The vibrational spectral data of isomeric benzaldehyde and dihydroxybenzaldehyde have been calculated based on normal coordinate analysis by Singh etal.[8]. Although much work has been done on substituted benzaldehydes, a comprehensive study of EHB on electronic structure along with the detailed potential energy distribution of normal modes of vibrations has not been reported so far. In the present study, the molecular structure, geometric parameters and vibrational frequencies of EHB are calculated using HF/6-31G (d, p), B3LYP/6-31++G (d, p) and B3LYP/6-311++G (d, p) basis sets and compared with the experimental data. The redistribution of electron density (ED) in various bonding, anti-bonding orbitals and E(2) energies have been calculated by Natural Bond Orbital (NBO) analysis to give clear evidence of

stabilization originating from the hyper conjugation of various intra-molecular interactions. HOMO-LUMO analysis has been used to elucidate information regarding charge transfer within the molecule. The Molecular Electrostatic Potential (MEP), thermodynamic properties and Mulliken charge analysis have also been studied. The UV-Vis spectrum of EHB is measured in ethanol and water solvents.

EXPERIMENTAL

The 3-Ethoxy-4-hydroxy benzaldehyde compound was purchased from Sigma-Aldrich Company (USA) with a stated purity of 98% and it was used as such without further purification. The FT-IR spectrum of molecule was recorded in the region 4000-450cm^{-1} using Perkin Elmer RXI spectrometer. FT-Raman spectra were recorded in the range of 4000- 50cm^{-1} using BRUKER, model RFS spectrophotometer. The UV absorption spectra were recorded in ethanol and water solvents in the region 200-400 nm using Perkin Elmer LAMDA UV-Vis NIR spectrometer.

Computational Details

The DFT computation of EHB had been performed using Gaussian 03 program package[9] at HF method with 6-31G (d,p) and DFT (B3LYP) method with 6-31++G(d,p) and 6-311++G(d,p) basis sets. The optimized structural parameters were evaluated for the calculations of vibrational frequencies at different methods. The harmonic vibrational frequencies had been analytically calculated by taking the second order derivative of energy using the same level of theory. Normal co-ordinate analysis had been performed in order to obtain the detailed interpretation of the fundamental modes using the MOLVIB program version 7.0 written by Sundius[10, 11]. The scaling of the force field was performed according to the scaled quantum mechanical procedure (SQM)[12,13] using selective scaling in the natural internal co-ordinate representation[14, 15] to obtain a better agreement between the theory and the experiment. The Raman activities (S_i) calculated by the Gaussian 03W program and converted into relative Raman intensities (I_i) during the scaling program with MOLVIB using the following relationship was derived from the basic theory of Raman scattering[16, 17].

$$I_i = \frac{f(\nu_o - \nu_i)^4 S_i}{\nu_i \left[1 - \exp\left(\frac{-hc\nu_i}{kT}\right)\right]} \quad (1)$$

Where ν_0 is the exciting wave number (cm^{-1}) of laser light source used while recording Raman spectra, ν_i is the vibrational wave number of the ith normal mode; h, k, c and T are Planck and Boltzmann constants, speed of light and temperature in Kelvin respectively. F is the suitably chosen common normalization factor for all the peak intensities.

The NBO calculations[18] were performed using NBO 3.1 program as carried out in the Gaussian 03 W package at the DFT/B3LYP level in order to understand the various second order interactions between the filled orbitals and vacant orbitals.The electronic absorption spectra for optimized molecule were calculated with the time dependent density functional theory (TD-DFT) at B3LYP/6-311++G (d, p) level.

RESULTS AND DISCUSSION

Molecular geometry

The optimized geometry structure of the title compound is shown in Fig 1. The optimized bond lengths, bond angles and dihedral angles calculated by HF/6-31G(d,p) and DFT-B3LYP level with 6-31++G(d,p), 6-311++G(d,p) basis sets are compared with the experimental data and are presented in Table 1.In the substitution of the aldehyde and hydroxyl groups, the bond lengths C1-O8(1.213Å) and C5-O9(1.362Å) calculated by B3LYP/6-311++G(d,p) are in good agreement with the experimental values for the title

molecule and are close to the literature value[19] 1.208Å/1.359Å.The bond angle C2-C3-C4(121.41°) is larger than C3-C4-C5(118.694°) due to the substitution of ethoxy group.

Table-1: Experimental (XRD) and optimized geometrical parameters of EHB computed at HF/6-31G (d, p), B3LYP/6-31++G (d, p) and B3LYP/6-311++G (d, p) basis sets.

Geometric parameters	Experimental value	Calculated values		
		HF/6-31G(d, p)	B3LYP/6-31++G(d, p)	B3LYP/6-311++G(d, p)
Bond length(**Å**)				
C1-C2	1.46	1.478	1.475	1.475
C1-O8	1.211	1.192	1.221	1.213
C1-H13	1.009	1.096	1.112	1.111
C2-C3	1.397	1.392	1.404	1.4
C2-C7	1.382	1.388	1.404	1.4
C3-C4	1.378	1.378	1.392	1.389
C3-H14	1.004	1.076	1.087	1.085
C4-C5	1.403	1.396	1.412	1.409
C4-O10	1.359	1.356	1.371	1.368
C5-C6	1.385	1.389	1.403	1.399
C5-O9	1.349	1.344	1.364	1.362
C6-C7	1.376	1.381	1.389	1.386
C6-H15	0.983	1.077	1.088	1.087
C7-H16	0.923	1.074	1.085	1.083
O9-H17	0.814	0.943	0.967	0.964
O10-C11	1.433	1.417	1.446	1.445
C11-C12	1.503	1.513	1.517	1.515
C11-H18	1.012	1.084	1.095	1.093
C11-H19	0.99	1.088	1.099	1.097
C12-H20	0.964	1.086	1.095	1.093
C12-H21	0.986	1.084	1.094	1.092
C12-H22	0.994	1.084	1.094	1.092
Bond Angles(°)				
C2-C1-O8	124.54	124.551	125.021	125.115
C2-C1-H13	114.81	114.989	114.742	114.484
O8-C1-H13	120.63	120.461	120.237	120.4
C1-C2-C3	119.54	120.108	119.578	119.641
C1-C2-C7	120.59	120.573	121.039	120.999
C3-C2-C7	119.86	119.319	119.384	119.359
C2-C3-C4	120.38	121.199	121.338	121.41

C2-C3-H14	117.78	120.816	120.617	120.574
C3-C4-C5	119.18	119.073	118.757	118.694
C4-C3-H14	121.83	117.981	118.042	118.01
C3-C4-O10	126.72	120.205	119.477	119.543
C5-C4-O10	114.08	120.676	121.626	121.629
C4-C5-C6	120.14	119.993	120.078	120.057
C4-C5-O9	121.08	117.548	117.523	117.591
C6-C5-O9	118.78	122.459	122.398	122.349
C5-C6-C7	120.17	120.377	120.557	120.608
C5-C6-H15	117.13	119.408	119.178	119.12
C7-C6-H15	122.67	120.215	120.261	120.267
C2-C7-C6	120.24	120.039	119.878	119.865
C2-C7-H16	117.38	119.252	119.107	119.123
C6-C7-H16	122.37	120.709	121.015	121.011
C5-O9-H17	113.43	110.986	109.934	109.778
C4-O10-C11	118.12	116.376	116.555	116.619
O10-C11-C12	106.81	107.742	107.655	107.685
O10-C11-H18	106.87	109.747	109.558	109.524
O10-C11-H19	107.29	109.234	108.535	108.514
C12-C11-H18	113.33	110.885	111.116	111.125
C12-C11-H19	112.54	110.971	111.193	111.219
H18-C11-H19	109.61	108.248	108.737	108.724
C11-C12-H20	107.01	110.195	109.858	109.883
C11-C12-H21	103.18	110.593	110.891	110.877
C11-C12-H22	110.53	110.323	110.605	110.596
H20-C12-H21	113.43	108.591	108.478	108.456
H20-C12-H22	111.75	108.652	108.48	108.462
H21-C12-H22	110.53	108.429	108.461	108.498
Dihedral Angles(°)				
O8-C1-C2-C3	179.41	-179.454	-179.388	-179.354
O8-C1-C2-C7	0.54	0.601	0.477	0.517
H13-C1-C2-C3	0.94	0.528	0.597	0.635
H13-C1-C2-C7	-177.92	-179.418	-179.538	-179.494
C1-C2-C3-C4	178.19	-179.796	-179.859	-179.825
C1-C2-C3-H14	0.75	-0.564	-0.514	-0.525
C7-C2-C3-C4	0.69	0.15	0.272	0.302
C7-C2-C3-H14	179.63	179.383	179.618	179.602
C1-C2-C7-C6	177.65	179.729	179.685	179.693
C1-C2-C7-H16	-1.37	-0.074	-0.074	-0.058

C3-C2-C7-C6	-1.24	-0.218	-0.449	-0.436
C3-C2-C7-H16	179.76	179.98	179.792	179.813
C2-C3-C4-C5	0.76	0.129	0.497	0.399
C2-C3-C4-O10	179.34	177.686	176.269	176.274
H14-C3-C4-C5	-178.13	-179.125	-178.865	-178.918
H14-C3-C4-O10	0.45	-1.568	-3.093	-3.043
C3-C4-C5-C6	-1.72	-0.342	-1.094	-0.97
C3-C4-C5-O9	177.97	179.757	178.492	178.507
O10-C4-C5-C6	179.53	-177.887	-176.772	-176.755
O10-C4-C5-O9	-0.79	2.212	2.814	2.722
C3-C4-O10-C11	4.44	102.601	113.649	113.424
C5-C4-O10-C11	-176.92	-79.882	-70.703	-70.826
C4-C5-C6-C7	1.21	0.278	0.933	0.85
C4-C5-C6-H15	179.43	-179.992	-179.849	-179.942
O9-C5-C6-C7	178.48	-179.827	-178.632	-178.602
O9-C5-C6-H15	-0.26	-0.097	0.585	0.606
C4-C5-O9-H17	3.94	-177.929	-178.245	-178.107
C6-C5-O9-H17	-176.38	2.173	1.33	1.358
C5-C6-C7-C2	0.26	0.005	-0.151	-0.137
C5-C6-C7-H16	179.23	179.804	179.603	179.609
H15-C6-C7-C2	-177.86	-179.723	-179.359	-179.336

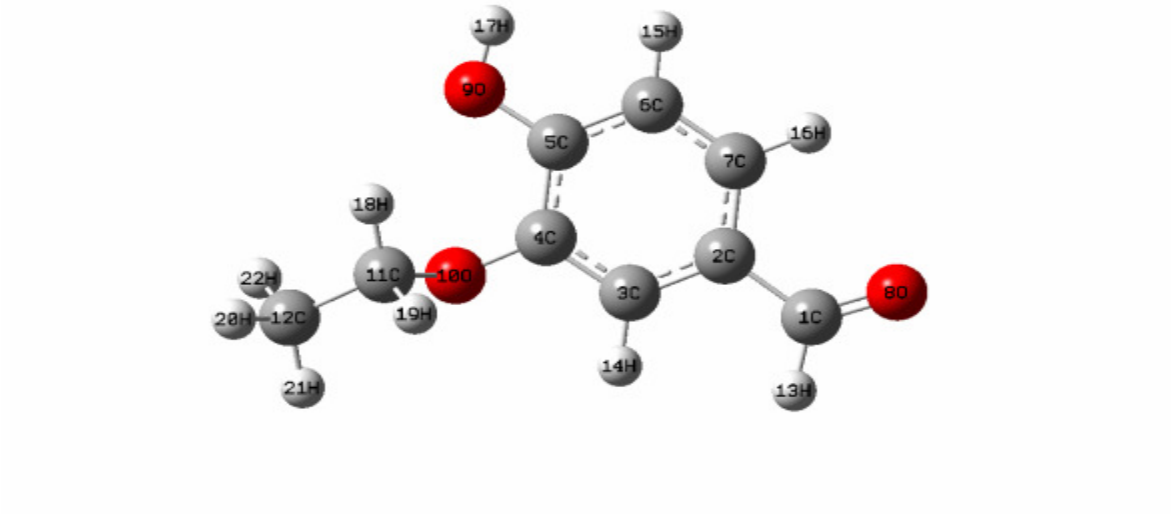

Fig.-1: Molecular structure with atom numbering of EHB.

Vibrational analysis

A detailed vibrational description has been carried out with the help of normal coordinate analysis. Internal coordinates have been described according to Pulay's recommendations. A non-redundant set of local symmetry coordinates constructed by suitable linear combinations of internal coordinates suggested by Rahut and Pulayand are presented in Table2. Vibrational frequencies have been calculated using HF/6-

31G (d, p), B3LYP/6-31++G (d, p) and B3LYP/6-311++G (d, p) basis sets. The calculated FT-IR and Raman vibrational wave numbers and assignments of EHB are given in Table 3, along with the experimental values. The experimental and theoretical FT-IR and FT-Raman spectra of the title compound are shown in Figs 2 and 3.

Table-2: Definition of local symmetry coordinates for EHB

S. No.	Symmetry Co-ordinates[a]	Description [b]
1	$S_1= r_{2\ 3}$	υC2C3
2	$S_2= r_{3\ 4}$	υC3C4
3	$S_3= r_{4\ 5}$	υC4C5
4	$S_4= r_{5\ 6}$	υC5C6
5	$S_5= r_{6\ 7}$	υC6C7
6	$S_6= r_{7\ 2}$	υC7C2
7	$S_7= r_{3\ 14}$	υC3C14
8	$S_8= r_{6\ 15}$	υC6C15
9	$S_9= r_{7\ 16}$	υC7 C16
10	$S_{10}= r_{1\ 13}$	υC1C13
11	$S_{11}= r_{5\ 9}$	υC5O9
12	$S_{12}= r_{4\ 10}$	υC4O10
13	$S_{13}= r_{2\ 1}$	υC2C1
14	$S_{14}= r_{1\ 8}$	υC1O8
15	$S_{15}= r_{11\ 10}$	υC11O10
16	$S_{16}= r_{9\ 17}$	υO9H17
17	$S_{17}= r_{11\ 12}$	υC11C12
18	$S_{18}= r_{11\ 18}+r_{11\ 19}$	υCH_2ss
19	$S_{19}= r_{11\ 18}- r_{11\ 19}$	υCH_2as
20	$S_{20}= r_{12\ 20}+ r_{12\ 21}+r_{12\ 22}$	υCH_3ss
21	$S_{21}= 2r_{12\ 20} - r_{12\ 21} - r_{12\ 22}$	υCH_3ips
22	$S_{22}= r_{12\ 21} - r_{12\ 22}$	υCH_3ops
23	$S_{23}= \beta_{21\ 12\ 20}+ \beta_{21\ 12\ 22}+ \beta_{22\ 12\ 20}- \beta_{11\ 12\ 20}- \beta_{11\ 12\ 21}- \beta_{11\ 12\ 22}$	υCH_3sb
24	$S_{24}= 2\beta_{21\ 12\ 20}- \beta_{21\ 12\ 22}- \beta_{22\ 12\ 20}$	υCH_3ipb
25	$S_{25}= \beta_{21\ 12\ 22}- \beta_{22\ 12\ 20}$	υCH_3opb
26	$S_{26}= 2\beta_{11\ 12\ 20}- \beta_{11\ 12\ 21}- \beta_{11\ 12\ 22}$	υCH_3ipr
27	$S_{27}= \beta_{11\ 12\ 21} - \beta_{11\ 12\ 22}$	υCH_3opr
28	$S_{28}= \beta_{18\ 11\ 19}+ \beta_{12\ 11\ 10}$	CH_2sc
29	$S_{29}= \beta_{12\ 11\ 18}+ \beta_{10\ 11\ 18} - \beta_{12\ 11\ 19} - \beta_{10\ 11\ 19}$	CH_2wa
30	$S_{30}= \beta_{12\ 11\ 18}+\beta_{10\ 11\ 19} - \beta_{10\ 11\ 18} - \beta_{12\ 11\ 19}$	CH_2tw
31	$S_{31}= \beta_{12\ 11\ 18}+\beta_{12\ 11\ 19} - \beta_{10\ 11\ 18} - \beta_{10\ 11\ 19}$	CH_2ro
32	$S_{32}= \beta_{12\ 11\ 10} - \beta_{18\ 11\ 19}$	βCCOsc
33	$S_{33}= \beta_{15\ 6\ 5} - \beta_{15\ 6\ 7}$	βC6H15
34	$S_{34}= \beta_{16\ 7\ 6} -\beta_{16\ 7\ 2}$	βC7H16

35	$S_{35}= \beta_{14\,3\,2} - \beta_{14\,3\,4}$	βC3H14
36	$S_{36}= \beta_{9\,5\,6} - \beta_{9\,5\,4}$	βC5O9
37	$S_{37}= \beta_{10\,4\,5} - \beta_{10\,4\,3}$	βC4O10
38	$S_{38}= \beta_{1\,2\,7} - \beta_{1\,2\,3}$	βC1C2
39	$S_{39}= \beta_{4\,10\,11}$	βC4O10C11
40	$S_{40}= \beta_{17\,9\,5}$	βC5O9H17
41	$S_{41} = \beta_{13\,1\,2} - \beta_{13\,1\,8}$	βC1H13
42	$S_{42} = \beta_{2\,1\,8} - \beta_{13\,1\,2} - \beta_{13\,1\,8}$	βC2H13C1
43	$S_{43} = \beta_{4\,3\,2} - \beta_{3\,2\,7} + \beta_{2\,7\,6} - \beta_{7\,6\,5} + \beta_{6\,5\,4} - \beta_{5\,4\,3}$	βring1
44	$S_{44} = 2\,\beta_{4\,3\,2} - \beta_{3\,2\,7} + \beta_{2\,7\,6} + 2\,\beta_{7\,6\,5} - \beta_{6\,5\,4} - \beta_{5\,4\,3}$	βring2
45	$S_{45} = \beta_{3\,2\,7} - \beta_{2\,7\,6} + \beta_{6\,5\,4} - \beta_{5\,4\,3}$	βring 3
46	$S_{46} = \gamma_{7\,5\,6\,15}$	γ C6H15
47	$S_{47} = \gamma_{2\,6\,7\,16}$	γ C7H16
48	$S_{48}= \gamma_{2\,4\,3\,14}$	γ C3H14
49	$S_{49}= \gamma_{9\,5\,6\,4}$	γ C5O9
50	$S_{50}= \gamma_{10\,4\,5\,3}$	γ C4O10
51	$S_{51}= \gamma_{1\,2\,7\,3}$	γ C1C2
52	$S_{52}= \gamma_{13\,1\,2\,8}$	γ C1H13
53	$S_{53}=\tau_{4\,3\,2\,7} - \tau_{3\,2\,7\,6} + \tau_{2\,7\,6\,5} - \tau_{7\,6\,5\,4} + \tau_{6\,5\,4\,3} - \tau_{5\,4\,3\,2}$	τring 1
54	$S_{54}= 2\tau_{3\,2\,7\,6} - \tau_{4\,3\,2\,7} - \tau_{2\,7\,6\,5} + 2\,\tau_{6\,5\,4\,3} - \tau_{7\,6\,5\,4} - \tau_{5\,4\,3\,2}$	τring 2
55	$S_{55}=\tau_{4\,3\,2\,7} - \tau_{2\,7\,6\,5} + \tau_{7\,6\,5\,4} - \tau_{5\,4\,3\,2}$	τring 3
56	$S_{56}= \gamma_{10\,11\,12\,22} + \gamma_{10\,11\,12\,21} + \gamma_{10\,11\,12\,20}$	τCH_3
57	$S_{57}= \gamma_{4\,10\,11\,18} + \gamma_{4\,10\,11\,19}$	τCH2
58	$S_{58}= \gamma_{17\,9\,5\,6} + \gamma_{17\,9\,5\,4}$	τO9H17
59	$S_{59}= \gamma_{11\,10\,4\,5} + \gamma_{11\,10\,4\,3}$	τO10C11
60	$S_{60}= \gamma_{13\,1\,2\,7} + \gamma_{8\,1\,2\,7}$	τC1O8H13

[a]Atom numbering as in Fig.-1.

[b]Definitions are made in terms of the standard valence coordinates: $r_{i\,j}$ is the bond length between atoms i and j: β_{ijk} is the valence angle between i,j,k where j is the central atom: γ_{ijkl} is the out-of-plane angle between the i-j bond and the plane defined by the j.k.l atoms: τ_{ijkl} is the torsion (dihedral)angle between the plane defined by i,j,k and j,k,l atoms: a = cos 144° and b = cos 72°
(υ)stretching:(β)in-plane-bending:(γ)out-of-plane-bending:(τ)torsion.

C – H vibrations

In substituted benzene rings, the C-H stretching vibrations [20] give rise to bands at 3120- 3000 cm^{-1}. The C-H vibrations of the title compound are observed at 3089, 3065 and 3024cm^{-1} in the FT-IR spectrum and at 3088, 3068 and 3028cm^{-1} in the FT-Raman spectrum. The corresponding calculated wave numbers at 3074, 3043, 3023cm^{-1} and at 3085, 3061, 3036$cm^{-1}$and at 3087, 3063, 3039cm^{-1} by HF/6-31G (d,p), B3LYP/6-31++G(d,p) and B3LYP/6-311++G(d,p) levels respectively, show good agreement with observed bands of EHB. The in- plane aromatic C-H deformation vibrations[21] occur in the region 1300-1000cm^{-1}. The bands are sharp but are of weak to medium intensity. The medium and strong intensity bands at 1197 and 1041cm^{-1} in the FT-IR spectrum and at 1198 cm^{-1} in the FT-Raman spectrum are due to in-plane deformations. The C-H in-plane bending vibrations are calculated at 1209, 1083, 1046cm^{-1} by

HF/6-31G (d,p) and at 1196, 1074 ,1040cm^{-1}and at 1209, 1071, 1051cm^{-1}by B3LYP/31++G(d,p) and B3LYP/311++G(d,p) levels respectively. Bands involving the out-of-plane hydrogen bending vibrations [22] absorb in the range 1000 cm^{-1}to675cm^{-1}. The C-H out-of-plane bending vibrations are calculated at 915, 862, 830cm^{-1}by HF/6-31G (d, p) and at 913, 872, 833cm^{-1} and 904, 847, 818cm^{-1} by B3LYP/6-31++G (d, p), B3LYP/6-311++G (d, p) basis sets respectively. The observed peaks at 903, 852 and 839cm^{-1} in the FT-IR spectrum due to C-H out-of-plane bending vibrations are in good agreement with the calculated values by HF/6-31G(d,p), B3LYP/6-31++G(d,p) and B3LYP/6-311++G(d,p) basis sets.

C – C vibrations

The ring carbon – carbon stretching vibrations occur in the region 1625-1430 cm^{-1}. In general, the bands are of variable intensity and are observed at 1625-1590 cm^{-1}, 1590- 1575cm^{-1}, 1540-1470cm^{-1}, 1465-1430cm^{-1} and 1380-1280cm^{-1} from the frequency ranges given by Varsanyi[23], for the five bands in the region. In the present work, the frequencies observed in the FT-IR spectrum at 1603, 1578, 1515 and 1398 cm^{-1} and at 1602, 1577 and 1517cm^{-1} in the Raman spectrum have been assigned to C – C stretching vibrations. The theoretically computed values at 1615,1592, 1502, 1415, 1356, 1320cm^{-1} by HF/6-31G(d,p) and at 1599, 1586,1497,1411, 1346, 1305 cm^{-1} by B3LYP/6-31++G(d,p) and at 1589, 1574, 1502, 1411, 1333, 1309 cm $^{-1}$ by B3LYP/6-311++G(d,p) method for C-C vibrational modes give good agreement with the experimental data. The weak bands observed at 737 and 634cm^{-1} in the FT-IR and at 735, 635 and 461cm^{-1} in the FT-Raman are assigned to CCC deformations of phenyl ring. The calculated values are at 747, 642,456cm^{-1} by HF/6-31G (d, p) and at 740, 635, 455cm^{-1} by B3LYP/6-31++G (d, p) method.

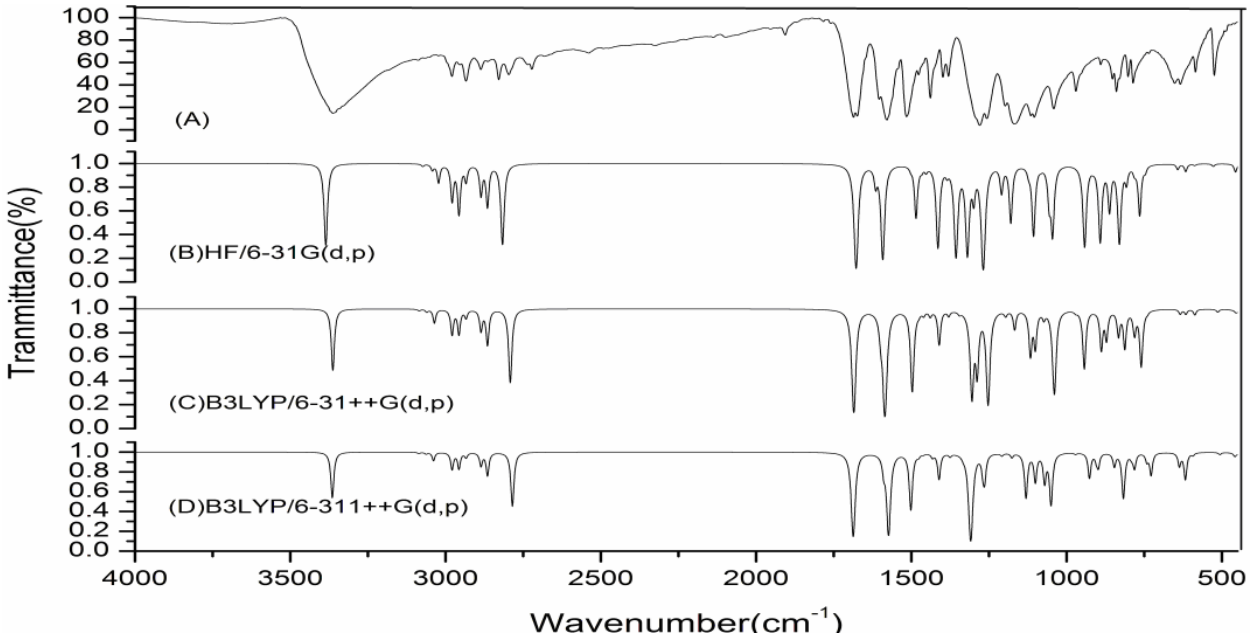

Fig.-2: Experimental (A), Simulated (B),(C) and (D) Infrared spectra of EHB at HF/6-31G(d,p),B3LYP/6-31++G(d,p) and B3LYP/6-311++G(d,p) levels.

Aldehyde group vibrations

The C-H stretching vibrations of aldehyde group[24] usually appear in the region 2806-2871cm^{-1}. In the present work, the weak band observed in the FT-IR spectrum at 2796cm^{-1} is due to the C-H stretching vibration of the aldehyde group. The C-H stretching vibration computed at 2817cm^{-1}by HF/6-31G(d,p) and at 2792cm^{-1} by B3LYP/6-31++G(d,p) method and at 2785cm^{-1}by B3LYP/6-311++G(d,p) for EHB shows good agreement with the recorded value. The in-plane CH deformation mode of aldehyde group occurs at 1300cm^{-1}. In EHB, the in-plane CH deformation mode of aldehyde group is observed at

1043cm^{-1}with weak intensity in the FT-Raman spectrum. The calculated wave number at 1056cm $^{-1}$ by HF/6-31G(d, p) and at 1044cm^{-1} by B3LYP/6-31++G(d,p) and at 1059cm^{-1}by B3LYP/6-311++G(d,p) method is attributed to CH in-plane deformation mode. The carbonyl(C=O) stretching vibrations[25] in the substituted benzaldehydes are reported near 1700cm^{-1}. The strong band centred at 1686cm^{-1} in the FT-IR and at 1684cm^{-1} in the FT-Raman are attributed to the C=O stretching vibrations of the aldehyde group of EHB. The theoretically calculated value is at1678cm^{-1} by HF/6-31G (d, p) and at 1686cm^{-1} by B3LYP/6-31++G (d, p) and at 1687cm^{-1} by B3LYP/6-311++G (d, p) method. Singh et al. [9] have assigned the C=O in-plane bending vibrations for methoxybenzaldehydes in the region 585-620cm^{-1}. Hence the weak band observed at 585cm^{-1}in the FT-IR and at 587cm^{-1} in the FT-Raman spectrum could be assigned to C=O in plane bending vibration. The calculated value is at 588cm^{-1} by HF/6-31G (d, p) and B3LYP/6-31++G (d, p) methods and at 593cm^{-1} by B3LYP/6-311++G (d, p) method. Gunasekaran et al.[26] have assigned the band at 188cm^{-1} in the Raman spectrum of 3-methoxy-4-hydroxybenzaldehyde as aldehyde out-of-plane wag. In EHB, the weak band centred at 183cm^{-1} in the Raman spectrum could be due to aldehyde out-of-plane wagging vibration. The theoretically computed value is at 197cm^{-1} by HF/6-31G (d, p) method and at 185cm^{-1} by both B3LYP/6-31++G (d, p), 6-311++G (d, p) basis sets. A weak to medium intensity band due to aldehyde group CHO deformation vibration[27] is found in the region 975-780cm^{-1}. The out of plane C-H deformation mode of aldehyde group is observed at 970cm^{-1} with medium intensity in the FT-IR spectrum and at 975cm^{-1} in the FT-Raman spectrum for EHB. The calculated value at971cm^{-1} by HF/6-31G (d, p), B3LYP/6-31++G (d, p) methods and at 972cm^{-1} by B3LYP/6-311++G (d, p) method agree well with the experimental values.

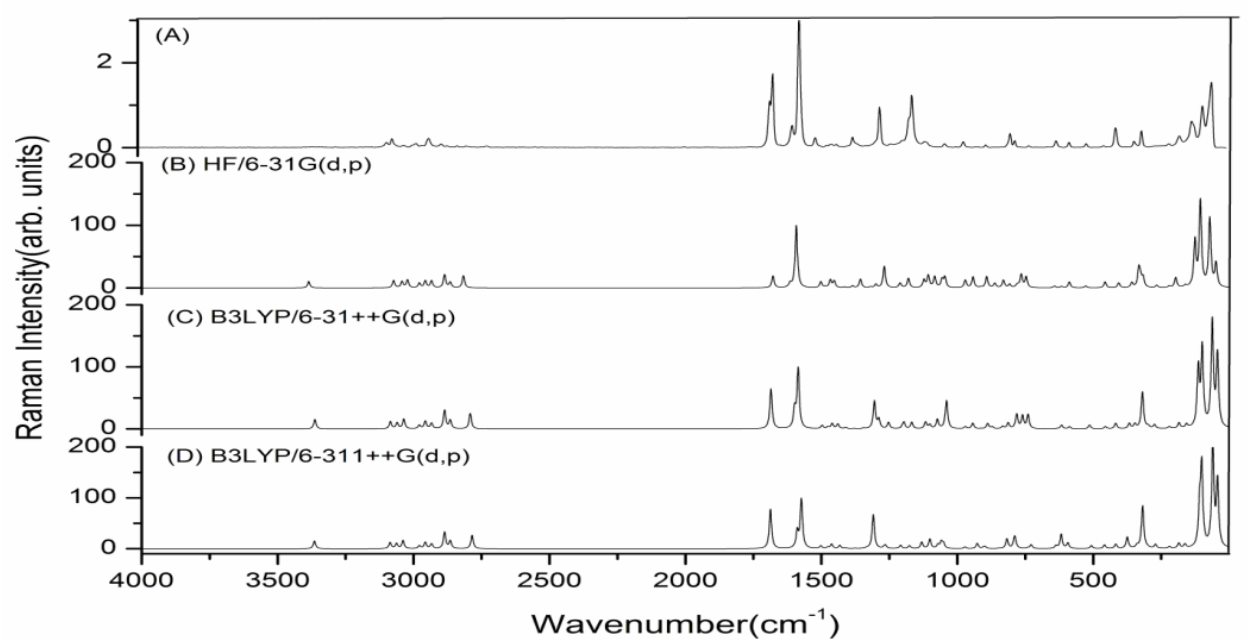

Fig.-3: Experimental (A), simulated (B), (C) and (D) Raman Spectra of EHB at HF/6-31G (d,p), B3LYP/6-31++G(d,p) and B3LYP/6-311++G(d,p) levels.

O – H vibrations

The OH group gives rise to three vibrations, namely, stretching, in-plane bending and out-of-plane bending. The precise position of O-H band depends on the strength of hydrogen bond. The O-H stretching[28] appears at 3500-3300 cm^{-1} in the intra-molecular hydrogen bonded systems. In the present work, the O-H stretching is found at 3363cm^{-1} in the FT-IR spectrum and calculated at 3386cm^{-1} by HF/6-31G(d,p) and at 3363, 3365cm^{-1} by B3LYP/6-31++G(d,p), 6-311++G(d,p) methods respectively. The in-plane bending vibration[29, 30] of OH occurs in the region 1400-1200cm $^{-1}$. The strong absorption at 1104cm^{-1} in FT-IR spectrum agrees well with the calculated wave number at 1107cm^{-1} by HF/6-31G(d, p)

and at 1101cm^{-1} by both B3LYP/6-31++G(d,p) and B3LYP/6-311++G(d,p) methods. The out-of-plane bending mode of OH is assigned to a medium band at 524cm^{-1} in both FT-IR and FT-Raman spectra. The calculated wave number is at 528cm^{-1}by HF/6-31G (d,p) and at 514cm^{-1} by B3LYP/6-31++G(d, p) and at 507cm^{-1} by B3LYP/6-311++G(d,p) method.

Table-3: Comparison of the experimental (FT-IR and FT-Raman) wave numbers (cm^{-1}) and theoretical wave numbers (cm-1) of EHB calculated by HF/6-31G (d. p), B3LYP/6-31++G (d, p) and B3LYP/6-311++G (d, p) basis sets.

Observed Wave numbers(cm^{-1})		Calculated by HF/6-31G(d, p)			Calculated by B3LYP/6-31++G(d, p)			Calculated by B3LYP/6-311++G(d, p)			Characterisation of normal modes with PED(%)[c]
IR	Raman	Scaled wave numbers(cm^{-1})	A_iIR^a	I_iR^b	Scaled wave numbers(cm^{-1})	A_iIR^a	I_iR^b	Scaled Wave numbers (cm^{-1})	A_iIR^a	I_iR^b	
3363(vs)		3386	115.8	100	3363	85.8	155.3	3365	91.9	146.2	υOH(100)
3089(w)	3088(w)	3074	2	83.8	3085	1.7	90	3087	1.8	88.8	υCH(99)
3065(w)	3068(w)	3043	5	69	3061	2.7	74	3063	2.5	72.9	υCH(99)
3024(w)	3028(w)	3023	17	85.9	3036	14.7	116.7	3039	13.3	111.7	υCH(99)
2979(m)	2981(w)	2979	36.8	49.5	2979	28.6	39.9	2979	28.3	37.2	CH3ops(93),CH2as(6)
2957(w)	2959(w)	2957	54.8	71.6	2957	28	84	2957	26.8	81	CH3ips(97)
2934(m)	2934(w)	2934	14.9	70.1	2934	8.6	61	2934	7.8	59.5	CH2as(74), CH2ss(16)
2886(w)	2888(w)	2886	30.1	124.9	2886	23.5	190.1	2886	21.6	194.5	CH3ss(99)
2865(m)	-	2865	44.1	51.3	2865	42.4	85.5	2865	39.8	88.7	CH2ss(81), CH2as(18)
2796(m)	-	2817	113.7	108.5	2792	114.4	145.65	2785	117.1	146.3	υCHO(99)
1686(s)	1684(s)	1678	214.2	33.6	1686	240.2	122.1	1687	284.8	139.8	υCOd(86)
1603(w)	1602(w)	1615	17.2	10.3	1599	23.8	50	1589	26.6	52.1	υCC(66), βring1(10)
1578(s)	1577(vs)	1592	163.7	158.7	1586	271.8	162.6	1574	271.4	153	υCC(65), βring1(9)
1515(vs)	1517(w)	1502	2.7	13.6	1497	140.1	8.2	1502	128.9	8	υCC(48), υCO(30)
1477(w)	1478(w)	1485	59.5	2.6	1476	2.4	4.2	1477	4.1	3.3	CH2sc(81), CH3IPB(6)
-	1460(w)	1467	3.5	17	1460	4.3	12.4	1463	1.4	12.2	CH3ipb(63) CH3opb(16)
1439(s)	1441(w)	1453	4.4	14.4	1439	5.8	11.1	1432	6.4	8.4	CH3opb(68), CH3ipb(16)
1398(m)	-	1415	123	1.8	1411	41.5	2.9	1411	46.4	1.4	υCC(50),υCO(19)
1380(m)	1380(w)	1385	5.5	4.1	1380	5.4	0.9	1376	4.9	0.7	CH3sb(76), CH3ipb(13)
-	-	1356	154.3	16.8	1346	2.7	1.2	1333	3.1	1.7	υCC(80)
-	-	1320	149	1.8	1305	167.4	53.6	1309	338.6	77.1	υCC(32), υCC(20)
1279(s)	1281(s)	1299	31.3	6.2	1289	93.9	17.3	1270	26.9	2.7	CH2wa(36), υCO(20)
1257(s)	1240(w)	1269	223.5	37.2	1253	193	11.5	1265	45.7	6.6	υCOH(39), CH2ro(22)
-	-	1211	4	4.2	1202	0.4	3	1222	0.6	0.5	CH3opr(35), CH2tw(29)
1197(w)	1198(w)	1209	22.7	3.7	1196	5	10.4	1209	4.1	6.6	βCH(61), βHOC(10)
1168(s)	1163(s)	1180	67.2	14.6	1168	21	10.5	1176	6.9	5.8	CH2tw(48), CH2wa(45)
1115(s)	1117(w)	1123	5.7	10.9	1117	57.9	10.1	1131	90.9	11.5	CH3ipr(44), CCOsc(14)
1104(s)	-	1107	92.3	16.8	1101	45.3	5.8	1101	51.2	16.2	βHOC(41), βCH(39)
-	-	1083	1.4	14.5	1074	7.7	13.3	1071	52.7	6.4	βCH(48), υCC(19)
-	1043(w)	1056	38.2	10.3	1044	13.9	3.6	1059	0.4	10.6	βHC(87), βCH(5)
1041(m)	-	1046	92	13	1040	141.8	36.2	1051	112.7	7.9	βCH(36), υCC(33)
970(m)	975(w)	971	0.2	8.7	971	1.9	2.6	972	2.1	2.4	γHC(72), γCCar(12)
-	-	942	120.2	11.8	943	82.3	6.6	927	44.3	6.9	υCO1(34), βring1(21)
903(w)	-	915	1.2	0.6	913	0.5	0.4	904	10.3	1.3	γCH(76), γCO(9)
890(w)	893(w)	892	106.9	11.2	889	48.7	5.8	898	22.6	2.5	υCC1(44), βring(19)
852(w)	-	862	48.8	4.2	872	33.5	2	847	21.7	0.3	γCH(40), γring1(18)
839(m)	-	830	111	6.8	833	28.6	2.3	818	93.1	10.7	γCH(42), γCO(15)
802(m)	803(m)	808	15.1	3	813	46.3	5.4	793	3.3	1.6	γCO (28), γring1(20)
786(w)	786(w)	782	5.1	1	786	2.6	0.9	789	4.4	12.2	CH2ro(48), CH2wa(28)
-	-	778	1.8	1.7	781	25.7	12.2	782	24.8	0.7	γCH(49), υCC (14)
-	-	765	55.9	10.3	760	77.8	10.9	742	13.3	0.8	βring1(45), υCCar(18)
737(w)	735(w)	747	4.8	8.3	740	1.6	11.4	728	38.4	3.6	γring1(27), γ CO(20)
634(m)	635(w)	642	4.7	1.1	635	5	0.2	637	21.5	2.1	γring1(28), βring1(12)
-	-	617	6.6	0.9	617	5	2.4	618	47.4	10.6	βring1(41), γring1(21)
585(m)	587(w)	588	1.3	3.2	588	5.9	1.2	593	3.8	3.9	βCO(41), γCCar(25)
524(m)	524(w)	528	2.2	0.9	514	2.9	1.9	507	3.3	1.7	γCO(48), γring1(29)
-	461(w)	456	7.1	2.3	455	2.2	0.9	459	5.5	1.8	γring1(47), CCOsc(17)
-	417(m)	406	5.6	1.6	418	106.4	2	417	102.3	1.8	τOH(89), γring1(5)
-	-	358	6.2	1.3	367	10.4	1.5	375	5.4	4	βring1(44), υCCar(20)
-	349(w)	332	4.6	4.4	347	0.7	1.2	339	0.3	0.9	γring1(60), γOH(20)

-	322(w)	326	108.4	1.8	319	2	8.7	318	8	11.7	βCO(20), υCCar(11)
-	-	317	20.3	2	298	0.4	0.5	300	2.2	0.2	CCOsc(23), γring1(18)
-	-	267	1.9	0.4	275	2.7	0.7	271	3.7	0.8	βCO(40), γring1(16)
-	220(w)	221	1.7	0.2	220	0.8	0.3	220	1.2	0.3	τCH3(85), CH3opr(6)
-	183(w)	197	14	1	185	10.5	0.5	185	10	0.6	γCO(30), γring1(19)
-	138(m)	162	0.1	0.8	157	10.5	0.3	163	10.1	0.3	β CCar(55), βCHC(11)
-	-	126	2.8	2.1	114	1.3	2.4	109	2	1.6	γring1(68), βCOC(13)
-	98(m)	106	2.6	2.9	99	4.6	2.6	101	3	3.1	τOC(35), τCOH(22)
	65(s)	71	1.5	1.1	62	1.5	1.4	60	1.7	1.5	τOC(56), βCO(10)
	-	49	0.1	0.2	43	0.1	0.5	43	0.1	0.5	τCH2(74), βCO(11)

vs –very strong ; s – strong; m- medium; w – weak; as- asymmetric; ss – symmetric; υ – stretching; β –in-plane bending; γ – out-of- plane bending; τ – torsion; sci – scissoring; ro – rocking; wag – wagging; tw – twisting; sb – symmetric bending; ips – in-plane stretching; ops – out-of-plane stretching; ipb – in-plane bending; opb – out-of-plane bending; ipr – in-plane rocking; opr – out-of-plane rocking;

[a]Calculated IR intensities, [b]Raman activity.

Ethoxy vibrations

The five ethyl C-H stretching vibrations absorb between 2995 and 2855 cm^{-1} with a moderate to strong intensity. The normal vibrations are usually arranged in order of descending wave number $\nu_a Me \geq \nu_a^* Me \geq \nu_a CH_2 \geq \nu_s Me \geq \nu_s CH_2$. The CH_3 asymmetric stretching vibrations occur at 2975 – 2950cm^{-1} and may easily be distinguished from the nearby CH_2 absorption at about 2930cm^{-1}. The symmetric CH_3 stretching absorption band[31] occurs at 2885-2865cm^{-1} and that of the methylene group at 2870-2840cm^{-1}. In EHB, both the asymmetric and symmetric stretching vibrations of CH_3 group have been calculated at 2979, 2957 and 2886cm^{-1} by HF/6-31G (d, p) and B3LYP/6-31++G (d, p), 6-311++G (d, p) methods. The C-H asymmetric stretching vibrations of a CH_3 group are observed at 2979 and 2957cm^{-1} in the FT-IR and 2981 and 2959cm^{-1} in the FT-Raman spectra respectively while symmetric stretching vibration of CH_3 is assigned at 2886cm^{-1} in FT-IR and at 2888cm^{-1} in the FT-Raman spectrum of EHB. The presence of adjacent electronegative atoms or groups can alter the position of the methyl symmetric band significantly, its range being 1470-1260 cm^{-1} whereas the asymmetric band is far less sensitive its range being 1485-1400cm^{-1}. The asymmetrical methyl deformation modes are obtained at 1439cm^{-1} in the FT-IR and at 1460 and 1441cm^{-1} in the FT-Raman spectrum of EHB. The asymmetrical methyl deformation modes calculated at 1467, 1453cm^{-1} by the HF/6-31G (d, p), 1460, 1439cm^{-1} by the B3LYP/6-31++G (d, p) and 1463, 1432cm^{-1} by the B3LYP/6-311++G (d, p) methods, which show good agreement with the experimental values. The symmetrical methyl deformational mode of EHB assigned both in FT-IR and FT-Raman spectra at 1380cm^{-1},agrees well with the calculated values at 1385, 1380 and 1376cm^{-1} by HF/6-31G(d,p), B3LYP/6-31++G(d,p) and B3LYP/6-311++G(d,p) methods respectively. The CH_3 rocking vibration in ethoxy derivatives has been assigned to the region 1190-1108cm^{-1}. The rocking vibration of the CH_3 group has been calculated at 1123cm^{-1} by HF/6-31G(d,p) and at 1117cm^{-1} by B3LYP/6-31++G(d,p) and at 1131cm^{-1} by B3LYP/6-311++G(d,p) method. This vibration shows good agreement with FT-IR and FT-Raman recorded values at 1115cm^{-1} and 1117cm^{-1}. The CH_3 torsional mode[32] is expected in the region 235±25cm^{-1}. The observed wave number in FT-Raman at 220cm^{-1} assigned to the CH_3 torsional mode of EHB, shows good agreement with the computed wave number at 221$cm^{-1}$by HF/6-31G(d, p) and at 220cm^{-1} by both B3LYP/6-31++G(d,p), B3LYP/6-311++G(d,p) methods.

The CH_2 anti-symmetric stretching vibration is generally observed in the region 3000-2900cm^{-1}, while the CH_2 symmetric stretch[33, 34] will appear between 2900 and 2800cm^{-1}. The band at 2934cm^{-1} is assigned to CH_2 asymmetric stretching in both FT-IR and FT-Raman spectra which shows good agreement with the calculated value 2934cm^{-1} by HF/6-31G(d,p), B3LYP/6-31++G(d,p) and B3LYP/6-311++G(d,p) methods. The theoretically predicted value at 2865cm^{-1} by HF/6-31G (d, p), B3LYP/6-31++G (d, p) and B3LYP/6-311++G (d, p) methods is attributed to CH_2 symmetric stretching, which agrees well with the experimental value at 2865cm^{-1} in the FT-IR spectrum. The fundamental CH_2 vibrations such as scissoring, wagging, twisting and rocking[35]appear in the frequency region 1500-800cm^{-1}. The scissoring mode of CH_2 group gives rise to a characteristic band at 1477cm^{-1} in the FT-IR and at 1478cm^{-1} in the FT-Raman spectrum of EHB, which agrees well with the calculated value at 1485cm^{-1} by HF/6-31G(d,p) and

at 1476, 1477cm^{-1}by B3LYP/6-31++G(d,p), 6-311++G(d,p) basis sets respectively. The methylene wagging mode in ethoxy compounds expected in the region 1350±40cm^{-1}is with moderate to strong intensity. In EHB, the wagging vibrational band of CH_2 mode is recorded at 1279 and 1281cm^{-1} as a strong and medium band in FT-IR and FT-Raman spectrum respectively and its corresponding calculated value is 1299cm^{-1}by HF/6-31G(d, p) and at 1289cm^{-1} by B3LYP/6-31++G(d,p) and at 1270cm^{-1} by B3LYP/6-311++G(d,p). The methylene twist is located in the region 1285±45cm^{-1} with a weak to moderate intensity. The CH_2 twisting mode in the FT-IR is observed at 1168cm^{-1} and at 1163cm^{-1} in the FT-Raman spectrum of EHB. The theoretically computed CH_2 twisting mode is at 1180cm^{-1} by HF/6-31G (d, p) and at 1168cm^{-1} by B3LYP/6-31++G(d,p) and at 1176cm^{-1} by B3LYP/6-311++G(d,p) method. The medium peak at 786cm^{-1} both in FT-IR and FT-Raman is assigned to the CH_2 rocking mode of EHB. The CH_2rocking mode predicted at 782cm^{-1}by HF/6-31G(d,p) and at 786cm^{-1}by B3LYP/6-31++G(d,p) and at 789cm^{-1} by B3LYP/6-311++G(d,p) method show excellent agreement with the experimental data.

Natural bond orbital (NBO) analysis

The NBO analysis is carried out by considering all possible interactions between filled donor and empty acceptor NBOs, and estimating their energetic importance by second-order perturbation theory. NBO analysis has been performed on the title molecule at the DFT/B3LYP/6-311++G (d, p) level in order to elucidate the intra-molecular and delocalization of electron density within the molecule. The hyper-conjugative interaction energy can be deduced from the second order perturbation approach.

$E^{(2)} = \Delta E_{ij} = q_i F(i,j)^2 / \varepsilon_j - \varepsilon_i$

Where q_i is the i^{th} donor orbital occupancy, ε_i,ε_j are diagonal elements (orbital energies) and F(i,j) is the off-diagonal NBO Fock-matrix element. The larger the $E^{(2)}$ value the more intensive is the interaction between electron donors and electron acceptors, i.e., more donating tendency from electron donors to electron acceptors and greater the extent of conjugation of the whole system .

Table-4: Second order perturbation theory analysis of fock matrix in NBO basis for EHB.

Donor(i)	ED(i)(e)	Acceptor (j)	ED (j) (e)	E(2)[a] (kcal/mol)	E(j)-E(i)[b] (a.u)	F(i,j)[c] (a.u)
σ(C1-C2)	1.98135	σ*(C2-C3)	0.02065	2.1	1.24	0.046
		σ*(C2-C7)	0.02461	2.01	1.24	0.045
		σ*(C3-C4)	0.02334	2.12	1.24	0.046
		σ*(C6-C7)	0.01316	2.24	1.25	0.047
π(C1-O8)	1.98075	π*(C2-C7)	0.3967	4.19	0.4	0.041
σ(C1-H13)	1.98643	σ*(C2-C7)	0.02461	4.25	1.1	0.061
σ(C2-C3)	1.97332	σ*(C2-C7)	0.02461	3.84	1.27	0.062
		σ*(C3-C4)	0.02334	2.56	1.27	0.051
		σ*(C4-O10)	0.02521	3.64	1.06	0.055
		σ*(C7-H16)	0.01425	2.23	1.15	0.045
σ(C2-C7)	1.97259	σ*(C2-C3)	0.02065	3.78	1.27	0.062
		σ*(C3-H14)	0.0144	2.5	1.13	0.048
		σ*(C6-C7)	0.01316	2.74	1.28	0.053
		σ*(C6-H15)	0.01424	2.75	1.11	0.049
π(C2-C7)	1.62097	π*(C1-O8)	0.12391	19.27	0.27	0.069
		π*(C3-C4)	0.3408	22.81	0.27	0.071
		π*(C5-C6)	0.39936	18.81	0.26	0.063

σ(C3-C4)	1.97499	σ*(C1-C2)	0.05878	2.94	1.17	0.053
		σ*(C2-C3)	0.02065	3.12	1.29	0.057
		σ*(C4-C5)	0.04274	3.36	1.25	0.058
		σ*(C5-O9)	0.02142	3.29	1.05	0.053
π(C3-C4)	1.67254	π*(C2-C7)	0.3967	17.01	0.29	0.064
		π*(C5-C6)	0.39936	22.37	0.28	0.072
σ(C3-H14)	1.97568	σ*(C2-C7)	0.02461	4.48	1.09	0.063
		σ*(C4-C5)	0.04274	4.04	1.06	0.059
σ(C4-C5)	1.9712	σ*(C3-C4)	0.02334	3.35	1.29	0.059
		σ*(C3-H14)	0.0144	2.14	1.15	0.044
		σ*(C5-C6)	0.02473	3.58	1.26	0.06
		σ*(C6-H15)	0.01424	2.04	1.13	0.043
σ(C5-C6)	1.97773	σ*(C4-C5)	0.04274	3.68	1.25	0.061
		σ*(C4-O10)	0.02521	3.37	1.08	0.054
		σ*(C6-C7)	0.01316	3.02	1.31	0.056
		σ*(C7-H16)	0.01425	2.18	1.17	0.045
π(C5-C6)	1.63738	π*(C2-C7)	0.3967	23.42	0.3	0.075
		π*(C3-C4)	0.3408	16.17	0.29	0.062
σ(C6-C7)	1.97575	σ*(C1-C2)	0.05878	3.18	1.17	0.055
		σ*(C2-C7)	0.02461	2.99	1.28	0.055
		σ*(C5-C6)	0.02473	2.78	1.25	0.053
		σ*(C5-O9)	0.02142	4.12	1.05	0.059
σ(C6-H15)	1.97841	σ*(C2-C7)	0.02461	3.33	1.11	0.054
		σ*(C4-C5)	0.04274	3.91	1.07	0.058
σ(C7-H16)	1.97841	σ*(C2-C3)	0.02065	4.58	1.09	0.063
		σ*(C5-C6)	0.02473	3.61	1.06	0.055
σ(O9-H17)	1.98726	σ*(C4-C5)	0.04274	3.92	1.29	0.064
σ(C11-C12)	1.98935	σ*(C4-O10)	0.02521	2.35	0.98	0.043
σ(C11-H18)	1.98689	σ*(C12-H21)	0.00836	2.54	0.92	0.043
σ(C11-H19)	1.98672	σ*(C12-H22)	0,00819	2.52	0.92	0.043
σ(C12-H20)	1.9821	σ*(O10-C11)	0.02759	3.98	0.78	0.05
σ(C12-H21)	1.98846	σ*(C11-H18)	0.02433	2.39	0.9	0.042
σ(C12-H22)	1.98776	σ*(C11-H19)	0.02478	2.56	0.88	0.043
LP(1)O8	1.98477	σ*(C1-C2)	0.05878	1.4	1.15	0.036
		σ*(C1-H13)	0.06709	0.64	1.05	0.024
LP(2)O8	1.87853	σ*(C1-C2)	0.05878	17.46	0.72	0.102
		σ*(C1-H13)	0.06709	23.11	0.62	0.108
LP(1)O9	1.97865	σ*(C5-C6)	0.02473	5.84	1.16	0.074
LP(2)O9	1.86671	π *(C5-C6)	0.39936	28.09	0.35	0.095

LP(1)O10	1.95202	π *(C3-C4)	0.3408	2.22	0.52	0.033
		σ*(C4-C5)	0.04274	5.85	1.03	0.069
		σ*(C11-H18)	0.02433	3.02	0.9	0.047
LP(2)O10	1.90954	σ*(C3-C4)	0.02334	4.95	0.93	0.062
		π *(C3-C4)	0.3408	8.64	0.38	0.055
		σ*(C11-H19)	0.02478	5.54	0.75	0.058
π *(C5-C6)	0.39936	π *(C2-C7)	0.3967	190.66	0.02	0.083

The most important interaction in this molecule is electron donating from O9LP (2) to the anti-bonding π*(C5-C6) resulting in a stabilization of 28.09kcalmol^{-1}. All lone pair-bond pair interactions and bond pair-bond pair interactions with stabilization energy above 3kcalmol^{-1}are listed in Table 4. In EHB molecule, the bond pair donor orbital $\pi_{CC} \rightarrow \pi^*_{CC}$ interaction between the C5 – C6 bond pair and C2 – C7 anti-bonding orbital gives the strongest stabilization of 23.42kcalmol^{-1}. Likewise, π(C2-C7)→π*(C3-C4) and π(C3-C4)→ π*(C5-C6) interactions give strong stabilization energies 22.81 and 22.37kcalmol^{-1} respectively.O8LP(2) transfers the stabilization energy to σ*(C1-C2), σ*(C1-H13) with $E^{(2)}$ energy of about 17.46 and 23.11kcalmol^{-1} respectively as shown in Table 4.

Frontier molecular orbital analysis

The frontier molecular orbitals play an important role in the electric and optical properties. The highest occupied molecular orbitals (HOMOs) and the lowest-lying unoccupied molecular orbitals (LUMOs) are named as frontier molecular orbitals. The energy gap between HOMO and LUMO is very important in determining the chemical activity of the molecule. A small HOMO-LUMO energy gap implies low kinetic stability, because it is energetically favourable to add electrons to a low-lying LUMO and to receive electrons from a high-lying HOMO [36-38]. The energies of HOMO and LUMO and their orbital energy gaps are calculated using B3LYP/6-311++G(d,p) method and the pictorial illustration of the frontier molecular orbitals and their respective positive and negative regions are shown in the Fig 4for EHB. According to Fig.4, HOMO is mainly localized over the entire molecule except for methyl group. However, LUMO is characterized by a charge distribution on hydroxyl benzaldehyde except for ethoxy group. The HOMO→LUMO transition implies an electron density transfer from O atom. The HOMO and LUMO energies are - 0.24613 a.u. and - 0.07030a.u.in gas phase. The energy difference between the HOMO and LUMO is obtained as 0.17583a.u, which indicates the high stability of the molecule.

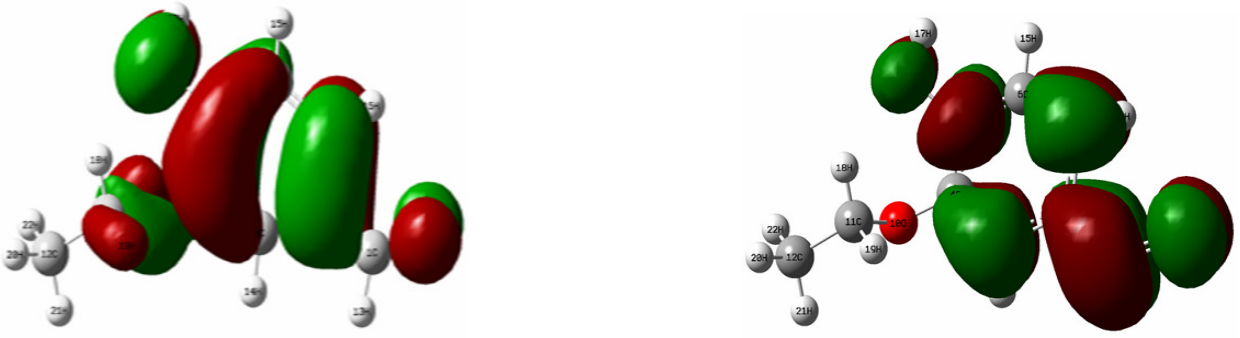

HOMO(-0.24430 a.u.) LUMO(-0.06934 a.u.)

Fig.-4: HOMO and LUMO plot of EHB

Molecular electrostatic potential

The MESP is a plot of electrostatic potential mapped onto the constant electron density surface and it simultaneously displays the molecular size, shape and electrostatic potential value in terms of colour coding. The total electron density mapped with the electrostatic potential surface of EHB constructed by the B3LYP/6-311++G(d,p) method is shown in Fig. 5. The MESP may be employed to distinguish regions on the surface which are electron poor (electrophilic attack) from those which are electron rich (nucleophilic attack). The different values of the electrostatic potential at the surface are represented by different colours; red represents the region of the most electronegative electrostatic potential, blue represents the region of the most positive electrostatic potential, green represents the region of zero potential and yellow represents slightly electron rich region. It is obvious from Fig. 5,that the region around the oxygen atom in the aldehyde group represents the negative potential region. The hydrogen atom attached in the hydroxyl group possesses positive charge. The predominance of green region in the ring surfaces and methyl group corresponds to a potential halfway between the two extremes red and blue colour. Hence the total electron density surface mapped with electrostatic potential reveals the presence of negative charge on the aldehyde oxygen while positive charge is present around the hydroxyl region.

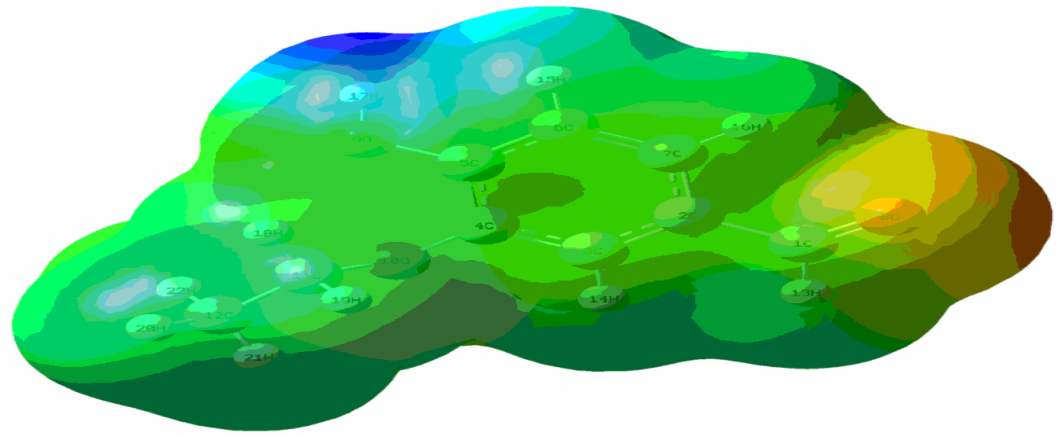

Fig.-5: Molecular electrostatic potential map of EHB calculated at B3LYP/6-311++G (d, p) level.

Thermodynamic properties

Theoretical geometrical parameters represent a good approximation and they are the basis for calculating vibrational frequencies and thermodynamic parameters. The frequency calculations compute the zero point energies, thermal correction to internal energy and entropy as well as the heat capacity for a molecular system. These functions describe the thermodynamic stability of the system at the given conditions of pressure and temperature. In order to clarify the relations among the energetic and structural reactivity of the title molecule, some calculated thermodynamic parameters (such as zero point vibrational energy, specific heat capacity, entropy, thermal energy, rotational constants and dipole moment) of EHB by DFT/B3LYP method at 298.15K and 1.00atmpressure are listed in Table5. On the basis of vibrational analysis and statistical thermodynamics, the standard thermodynamic functions heat capacity (C_p), entropy (S) and enthalpy (ΔH_m) are obtained and listed in Table6. As observed from the Table, the values of heat capacity, entropy and enthalpy increase with the increase of temperature from 100 to 1000K, which is attributed to the enhancement of molecular vibrations when the temperature increases.

According to the data in Table5 for the title compound, the correlations between the thermodynamic properties $C_{p,}$ S and ΔH_m and temperatures T are described and shown in Fig 6. The correlation equations of the title compound are as follows:

$C_p = 5.2969 + 0.15334\ T - 6.20388 \times 10^{-5}\ T^2$. ($R^2 = 0.99972$)

$S = 56.61203 + 0.18138\ T - 4.56742 \times 10^{-5}\ T^2$. ($R^2 = 0.99986$)

$\Delta H_m = -\ 3.26441 + 0.03036\ T - 3.19509 \times 10^{-5}\ T^2$. ($R^2 = 0.99585$)

Table-5: Thermodynamic properties at different temperatures at the B3LYP/6-311++G(d,p) level for EHB

Temperature (K)	Entropy (S) Cal/mol-Kelvin	Heat Capacity (Cp) cal/mol-Kelvin	Enthalpy(ΔHm) Kcal/mol
100	73.42	20.64	1.379
200	91.63	33.08	4.077
298.15	107.05	44.97	7.909
300	107.33	45.197	7.989
400	121.96	56.86	13.104
500	135.77	67.03	19.314
600	148.76	75.41	26.45
700	160.92	82.29	34.344
800	172.29	87.98	42.867
900	182.45	92.74	51.911
1000	192.92	96.77	56.612

Table-6: Theoretically computed zero point vibrational energy (kcal/mol), rotational constants (GHz), thermal energy (kcal mol^{-1}) and dipole moment for EHB

Total energy (thermal) kcal /mol	116.235
Vibrational energy kcal / mol	114.458
Zero point vibrational energy	108.92008
Rotational constants (GHz)	
A	1.87967
B	0.51928
C	0.41699
Dipole moment(Debye)	
μ_x	-3.6127
μ_y	2.0252
μ_y	1.4184
μ_{total}	4.3778

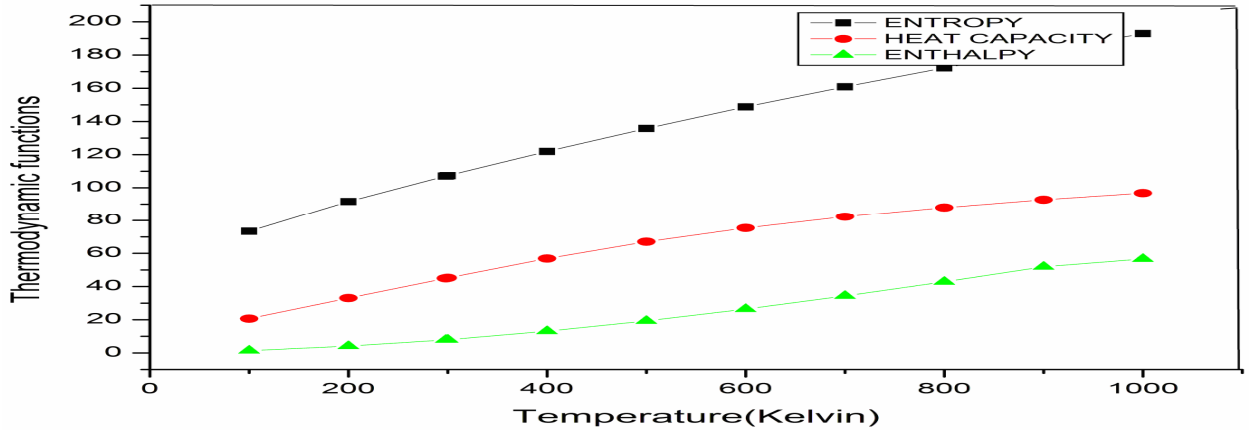

Fig.-6: Correlation graph of thermodynamic function (heat capacity, entropy and enthalpy) and temperature for EHB

Mulliken Atomic Charges

Mulliken population analysis is mostly used for the calculation of the charge distribution in a molecule[39]. Mulliken charges are calculated by determining the electron population of each atom as defined by the

basis set. The calculated mulliken charge values of EHB using the B3LYP/6-311++G (d,p) method are listed in Table.7. From Table 7, it is obvious that all the
hydrogen atoms have a net positive charge. The charge distribution of the title compound shows that the carbon atoms C3, C6 and C7 attached with hydrogen atoms are negative, whereas the remaining carbon atoms C2 and C5 are positively charged due to the substitution
of hydroxyl and aldehyde group. From the result, it is clear that the substitution of aromatic ring leads to a redistribution of electron density. The charge distribution on the molecule has an important influence on the vibrational spectra.[40]

Table-7: Mulliken Atomic Charges for EHB

Atoms	Charges
C1	-0.115
C2	0.928
C3	-0.497
C4	-0.608
C5	0.250
C6	-0.126
C7	-0.236
O8	-0.252
O9	-0.235
O10	-0.107
C11	-0.208
C12	-0.465
H13	0.128
H14	0.178
H15	0.140
H16	0.189
H17	0.276
H18	0.169
H19	0.140
H20	0.137
H21	0.152
H22	0.161

UV-Vis analysis

The ultraviolet spectra analyses of EHB have been investigated in water and ethanol solvents by theoretical calculation. On the basis of fully optimized ground state structure, TD-DFT/B3LYP/6-311++G (d,p) calculations have been used to determine the low-lying excited states of EHB. The theoretical electronic excitation energies, oscillator strengths and absorption wavelengths are listed in Table 8. Calculations of the molecular orbital geometry show that the absorption maxima of this molecule correspond to the electron transition between frontier orbitals such as transition from HOMO to LUMO. From Table.8, the calculated absorption maxima values have been found to be 228.51nm and 271.5nm for water solvent, 228.67nm and 271.26nm for ethanol solvent by B3LYP/6-311++G(d,p) method. The experimental results are observed at 233.6, 266.4nm and 233.4, 266.6nm for water and ethanol solvents respectively. These absorption maxima values are in good agreement with the theoretical values. The UV-Vis spectra of EHB were recorded in water and ethanol solvents as shown in Fig.-7.

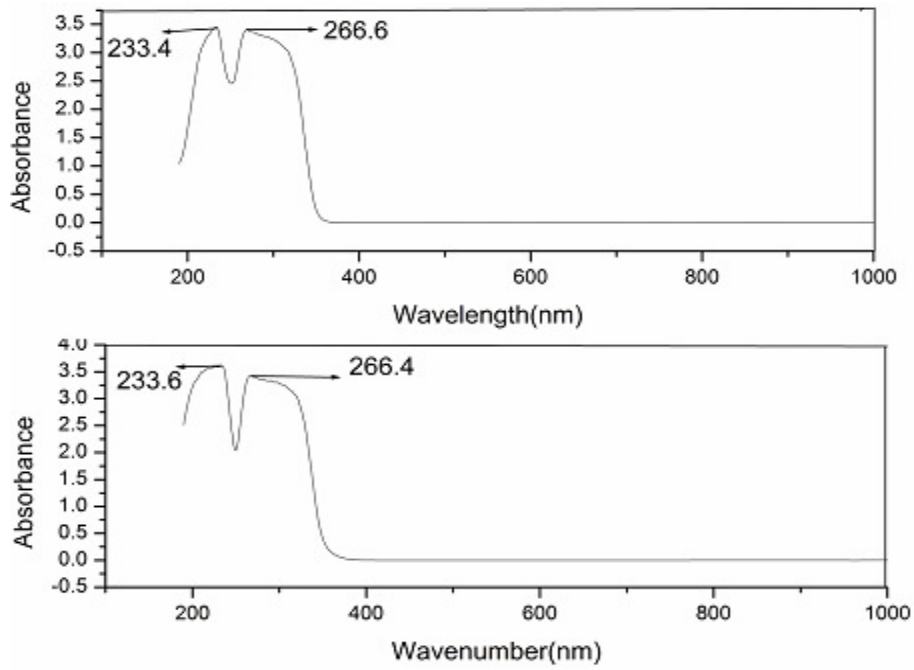

Fig.-7: Experimental UV-vis spectra of EHB in ethanol and water solvents.

Table-8: Theoretical electronic absorption spectra of EHB (absorption wavelength λ (nm), excitation energies E (ev) and oscillator strengths (f) using TD – B3LYP/6-311++G(d,p) method in water and ethanol solvents.

Experimental		Theoretical wavelength					
		Water			Ethanol		
Water	Ethanol	λ (nm)	E (ev)	f	λ (nm)	E (ev)	f
266.4	266.6	271.50	4.5667	0.1851	271.26	4.5707	0.1841
233.6	233.4	228.51	5.4258	0.3230	228.67	5.422	0.3308

CONCLUSIONS

Theoretical calculations have been carried out on 3 – Ethoxy – 4 – hydroxyl benzaldehyde(EHB) using HF/6-31G(d,p) and B3LYP/6-31++G(d,p), B3LYP/6-311++G(d,p) methods to explain the FT-IR and FT-Raman spectra and structural properties. The vibrational frequency analysis by the B3LYP/6-311++G(d,p) method agrees satisfactorily with the experimental results. The NBO result reflects the charge transfer within the molecule. Also the HOMO and LUMO energies of EHB in the ground state have been calculated by using the density functional theory. The large HOMO-LUMO energy gap indicates the high chemical stability of the molecule. The MESP map shows that the negative potential sites are on oxygen atoms in the methoxy group and the aldehyde group as well as the positive potential site is on the hydrogen atom in the hydroxyl group. The UV-vis spectrum of EHB was measured in ethanol and water solvents. The TD-DFT calculations show a good agreement with the observed values. The thermodynamic functions in the range from 100K to 1000K are obtained. The gradient of heat capacity, entropy and enthalpy increases with the increase of temperature.

REFERENCES

1. S.Gunasekaran and S.Ponnusamy , *Ind. J. Pure & Appl. Phys.,* **43,**838 (2005)
2. G.RamanaRao andA.Anjaneyulu , *Spectrochim Acta,***55A,**749 (1999)
3. T.Ikoh, N.Akai andK.Ohno ,*J. Mol. Struct.,***786,**39 (2002)
4. P.Venkata Ramana Rao and G.Ramana Rao ,*Spectrochim. Acta.,* **58A,** 3205 (2002)

5. N.Akai, S.Kudoh, M.Takayanagi and M.Nakara, *J. Photochem. Photobiol.*, **A150,**93(2002)
6. P.J.A.Ribeiro-Claro, M.P.M.Marques and A.M.Amado*, Chem. Phys. Chem.,***3,**599(2002)
7. P.Bednarek, T. Bally and J.Gebicki, *J. Org. Chem.,***67,**1319 (2002)
8. D.N.Singh, I.D. Singh and R A Yadav ,*Ind. J. Phys.,***763,**307 (2002).
9. M.J.Frisch, GAUSSIAN 03 Program, Gaussian, Inc.,Wattingford. CT.2004.
10. T.Sundius, *J.Mol. Struct.,***218,** 321 (1990)
11. T.Sundius,*Vib.Spectrosc*.,**29,** 89(2002)
12. G.Rauhut and P.Pulay, *J. Phys.Chem.*,**99,**3093 (1995)
13. P.Pulay, G.Fogarasi, G.Pongoe, J.E.Boggsand A.Vargha, *J. Am. Chem.Soc.,***105,**7037 (1983)
14. G.Fogarasi, P.Pulay and J.R.Durig(Eds.), *Vibrational Spectra and structure,***14,** Elsevier Publications. Amsterdam.(1985)
15. G. Fogarasi, N.Zhov, P.W. Taylor and P.Pulay, *J. Am. Chem.Soc.,***114,** 8191 (1992).
16. G.Keresztury, *Spectrochim Acta,* **A49,** 2007 (1993)
17. G.Keresztury, in: J.M. Chalmers and P.R. Griffith(Eds.),Raman Spectroscopy; Theory Handbook of Vibrational Spectroscopy,**Vol. 1,** John Wiley and Sons Ltd. New York, 71 (2002)
18. E.D.Glendening, A.E.Reed, J.E.Carpenter and F.Weinhold, NBO Version 3.1 TCI, University of Wisconsin, Medison, 1998.
19. P.Sykes, A Guidebook to Mechanism In Organic Chemistry, pp 15, Sixth Edition, Longman Publishing Group(1986).
20. M.Fatima Beegum, L.UshaKumari, B.Harikumar, HemaTresa Varghese and C.Yohannan Panicker, *Rasayan J. Chem*.,**1(2)**,258 (2008)
21. V.Arjunan, P.S.Balamourougane,C.V.Mythili and S.Mohan, *J. Mol. Struct.,***1003,**92(2011)
22. N.B.Colthup, L.H.Daly and S.E.Wiberley, Introduction to Infrared and Raman Spectroscopy, Third ed., Academic Press, Boston, (1990)
23. G.Varsanyi, Vibrational spectra of Benzene Derivatives, Academic Press, New York,(1969)
24. Syed Tariq, P.K.Verma and Rashid Aquell, *Indian J. Pure & Appl. Phys.*, **20,**974(1982)
25. V.Molnar, F.Billes, E.Tyihak and H.Mikosch, *Spectrochim. Acta.,***69A,**542(2008)
26. S.Gunasekaran and S.Ponnusamy, *Indian J. Pure & Appl.Phys.*, **43,**838 (2005)
27. G.Socrates, Infrared Characteristic group frequencies (John-Wiley & Sons, New York)(1980)
28. S.Kalaichelvan and N.Sundaraganesan, B.Dominic Joshua, *Indian Journal of Chemistry,***47A,**1632 (2008)
29. George Socrates Infrared and Raman Characteristic Group Frequencies - Tables and Charts*,*third ed., John Wiley & Sons, Chichester, (2001)
30. N.P.G.Roeges, A Guide to complete Interpretation of the Infrared Spectra of Organic Structures,Wiley, New York.(1954)
31. L.Usha Kumari, M.Fatima Beegum, B.Harikumar, Hema Tresa Varghese and C.Yohannan Panicker, *Rasayan J. Chem*., **1(2)**,246 (2008)
32. M.Arivazhagan, N.K.Kandasamy and G. Thilagavathi, *Indian J. Pure & Appl.Phys.,***50,**299(2012)
33. D.Sajan, J.Binoy, B.Pradeep, K.Venkatakrishnan,V.B.Kartha and I. H Joe, V.S. Vijayakumar, *Spectrochim. Acta,* **60A,**173(2004)
34. S.Gunasekaran, S.R.Varadhan and K.Manoharan, *Asian J. Phys*.,**2,**165 (1993)
35. Y.Erdogdu and M.TahilGulloeghi,*Spectrochim Acta* **A,74,**162 (2009)
36. M.D.Diener and J.M. Alford, *Nature,* **393,**668 (1998)
37. S.H.Yang, C.L.Pettiette,J.Conceicao,O.Cheshnovsky and R.E.Smalley, *Chem. Phys. Lett.,***139,**233 (1987)
38. H.Handschuh, G.Gantefor, B.Kessler, P.S.Bechthold and W.Eberhardt, *Phys Revlett*.**, 74,**1095(1995)
39. G.Raja, K.Saravanan and S. Sivakumar, *Rasayan J. Chem.,* **8(1),** 8(2015)
40. R.S.Mulliken, *J. Chem. Phys.,***23,**1831(1955)

[RJC-1317/2015]